

## Latin Americans show wide-spread *Converso* ancestry and the imprint of local Native ancestry on physical appearance

Juan C. Chacón-Duque<sup>1</sup>, Kaustubh Adhikari<sup>1</sup>, Macarena Fuentes-Guajardo<sup>1,2</sup>, Javier Mendoza-Revilla<sup>1,3</sup>, Victor Acuña-Alonzo<sup>1,4</sup>, Rodrigo Barquera Lozano<sup>4,5</sup>, Mirsha Quinto-Sánchez<sup>6</sup>, Jorge Gómez-Valdés<sup>7</sup>, Paola Everardo Martínez<sup>8</sup>, Hugo Villamil-Ramírez<sup>9</sup>, Tábita Hünemeier<sup>10</sup>, Virginia Ramallo<sup>11,12</sup>, Caio C. Silva de Cerqueira<sup>12</sup>, Malena Hurtado<sup>3</sup>, Valeria Villegas<sup>3</sup>, Vanessa Granja<sup>3</sup>, Mercedes Villena<sup>13</sup>, René Vásquez<sup>14</sup>, Elena Llop<sup>15</sup>, José R. Sandoval<sup>16</sup>, Alberto A. Salazar-Granara<sup>16</sup>, Maria-Laura Parolin<sup>17</sup>, Karla Sandoval<sup>18</sup>, Rosenda I. Peñalosa-Espinosa<sup>19</sup>, Hector Rangel-Villalobos<sup>20</sup>, Cheryl Winkler<sup>21</sup>, William Klitz<sup>22</sup>, Claudio Bravi<sup>23</sup>, Julio Molina<sup>24</sup>, Daniel Corach<sup>25</sup>, Ramiro Barrantes<sup>26</sup>, Verónica Gomes<sup>27,28</sup>, Carlos Resende<sup>27,28</sup>, Leonor Gusmão<sup>27,28,29</sup>, Antonio Amorim<sup>27,28,30</sup>, Yali Xue<sup>31</sup>, Jean-Michel Dugoujon<sup>32</sup>, Pedro Moral<sup>33</sup>, Rolando Gonzalez-José<sup>11</sup>, Lavinia Schuler-Faccini<sup>12</sup>, Francisco M. Salzano<sup>12</sup>, Maria-Cátira Bortolini<sup>12</sup>, Samuel Canizales-Quinteros<sup>9</sup>, Giovanni Poletti<sup>3</sup>, Carla Gallo<sup>3</sup>, Gabriel Bedoya<sup>34</sup>, Francisco Rothhammer<sup>15,35</sup>, David Balding<sup>1,36</sup>, Garrett Hellenthal<sup>1\*</sup> † and Andrés Ruiz-Linares<sup>37,38\*</sup> †

<sup>1</sup> Department of Genetics, Evolution and Environment and UCL Genetics Institute, University College London, London, UK.

<sup>2</sup> Departamento de Tecnología Médica, Facultad de Ciencias de la Salud, Universidad de Tarapacá, Arica, Chile.

<sup>3</sup> Laboratorios de Investigación y Desarrollo, Facultad de Ciencias y Filosofía, Universidad Peruana Cayetano Heredia, Lima, Peru.

<sup>4</sup> Molecular Genetics Laboratory, Escuela Nacional de Antropología e Historia, Mexico City, Mexico.

<sup>5</sup> Department of Archaeogenetics, Max Planck Institute for the Science of Human History, Jena, Germany.

<sup>6</sup> Ciencia Forense, Facultad de Medicina, Universidad Nacional Autónoma de México, Mexico City, Mexico.

<sup>7</sup> Posgrado en Antropología Física, Escuela Nacional de Antropología e Historia, Mexico City, Mexico.

<sup>8</sup> Posgrado en Antropología, Universidad Nacional Autónoma de México, Mexico City, Mexico.

<sup>9</sup> Unidad de Genómica de Poblaciones Aplicada a la Salud, Facultad de Química, Universidad Nacional Autónoma de México e Instituto Nacional de Medicina Genómica, Mexico City, Mexico.

<sup>10</sup> Departamento de Genética e Biología Evolutiva, Instituto de Biociências, Universidade de São Paulo, Sao Paulo, Brazil.

<sup>11</sup> Instituto Patagónico de Ciencias Sociales y Humanas-Centro Nacional Patagónico, CONICET, Puerto Madryn, Argentina.

<sup>12</sup> Departamento de Genética, Universidade Federal do Rio Grande do Sul, Porto Alegre, Brazil.

- <sup>13</sup> Instituto Boliviano de Biología de Altura (IBBA), Universidad Mayor de San Andrés (UMSA), La Paz, Bolivia.
- <sup>14</sup> Instituto Boliviano de Biología de Altura (IBBA), Universidad Autónoma Tomás Frías, Potosí, Bolivia.
- <sup>15</sup> Programa de Genética Humana, ICBM, Facultad de Medicina, Universidad de Chile, Santiago, Chile.
- <sup>16</sup> Facultad de Medicina Humana, Universidad de San Martín de Porres, Lima, Peru.
- <sup>17</sup> Instituto de Diversidad y Evolución Austral (IDEAus), Centro Nacional Patagónico, CONICET, Puerto Madryn, Argentina.
- <sup>18</sup> National Laboratory of Genomics and Biodiversity (LANGEBIO), CINVESTAV, Irapuato, Mexico.
- <sup>19</sup> Department of Biological Systems, Division of Biological and Health Sciences, Universidad Autónoma Metropolitana-Xochimilco, Mexico City, Mexico.
- <sup>20</sup> Instituto de Investigación en Genética Molecular, Universidad de Guadalajara, Ocotlán, Mexico.
- <sup>21</sup> National Cancer Institute, Frederick, MD, USA.
- <sup>22</sup> Integrative Biology, University of California, Berkeley, CA, USA.
- <sup>23</sup> Instituto Multidisciplinario de Biología Celular, CONICET, La Plata, Argentina.
- <sup>24</sup> Centro de Investigaciones Biomédicas de Guatemala, Ciudad de Guatemala, Guatemala.
- <sup>25</sup> Servicio de Huellas Digitales Genéticas and CONICET, Universidad de Buenos Aires, Buenos Aires, Argentina.
- <sup>26</sup> Escuela de Biología, Universidad de Costa Rica, San José, Costa Rica.
- <sup>27</sup> Instituto de Patología e Inmunología Molecular da Universidade do Porto (IPATIMUP), Porto, Portugal.
- <sup>28</sup> Instituto de Investigação e Inovação em Saúde (i3S), University of Porto, Porto, Portugal.
- <sup>29</sup> DNA Diagnostic Laboratory (LDD), State Universidade do Estado do Rio de Janeiro, Rio de Janeiro, Brazil.
- <sup>30</sup> Faculty of Sciences, University of Porto, Porto, Portugal.
- <sup>31</sup> The Wellcome Trust Sanger Institute, Hinxton, UK.
- <sup>32</sup> Centre National de la Recherche Scientifique, Université Toulouse 3 Paul Sabatier, Toulouse, France.
- <sup>33</sup> Departament de Biologia Animal-Antropologia, Universitat de Barcelona, Barcelona, Spain.
- <sup>34</sup> Genética Molecular (GENMOL), Universidad de Antioquia, Medellín, Colombia.
- <sup>35</sup> Instituto de Alta Investigación, Universidad de Tarapacá, Arica, Chile.
- <sup>36</sup> Schools of BioSciences and Mathematics & Statistics, University of Melbourne, Melbourne, Australia.
- <sup>37</sup> Ministry of Education Key Laboratory of Contemporary Anthropology and Collaborative Innovation Center of Genetics and Development, Fudan University, Shanghai, China.

<sup>38</sup> Aix-Marseille Univ, CNRS, EFS, ADES, Marseille, France.

\* Correspondence to: andresruiz@fudan.edu.cn (A.R.-L.); g.hellenthal@ucl.ac.uk (G.H.)

† Joint last authors

**Historical records and genetic analyses indicate that Latin Americans trace their ancestry mainly to the admixture of Native Americans, Europeans and Sub-Saharan Africans<sup>1</sup>. Using novel haplotype-based methods here we infer the sub-populations involved in admixture for over 6,500 Latin Americans and evaluate the impact of sub-continental ancestry on the physical appearance of these individuals. We find that pre-Columbian Native genetic structure is mirrored in Latin Americans and that sources of non-Native ancestry, and admixture timings, match documented migratory flows. We also detect South/East Mediterranean ancestry across Latin America, probably stemming from the clandestine colonial migration of Christian converts of non-European origin (*Conversos*). Furthermore, we find that Central Andean ancestry impacts on variation of facial features in Latin Americans, particularly nose morphology, possibly relating to environmental adaptation during the evolution of Native Americans.**

Genetic studies can provide refined insights into human population history. Recently developed haplotype-based methods have been shown to provide higher resolution than allele-based approaches for examining patterns of human population sub-structure<sup>2</sup>. A recent application of these methods enabled a detailed analysis of the population structure of the population of the British Isles, matching fine-grained historical events<sup>3</sup>. Other than contributing to historical reconstruction, a fine-grained analysis of patterns of population genetic sub-structure is of interest for assessing the genetic basis of geographic variation in human phenotypes. For instance, although the impact of continental ancestry on physical appearance is well established<sup>4</sup>, little is known about the genetic basis of variation in physical appearance within continental human populations. The inter-continental admixture history of Latin America makes it an ideal setting in which to examine patterns of sub-continental genetic structure, the historical correlates of this structure and its impact on physical appearance.

We examined data for over 500,000 autosomal SNPs typed in more than 6,500 individuals born in Brazil, Chile, Colombia, Mexico and Peru (denoted the CANDELA sample, Supplementary Fig. 1). To infer ancestry in this sample, we collated data for 2,359 individuals from 117 reference populations (including 430 newly genotyped individuals from 42 populations) representing five major bio-geographic regions: Native Americans; Europeans; East/South Mediterraneans; Sub-Saharan Africans and East Asians (Fig. 1A, Supplementary Table 1, Supplementary Fig. 2). We grouped the reference population individuals into 56 homogeneous clusters based on patterns of haplotype sharing, using the program fineSTRUCTURE<sup>2</sup> (Supplementary Tables 2 and 3). We inferred the proportion of the genome in each CANDELA individual that is most closely related to individuals in each of these 56 reference clusters, using a novel approach we term SOURCEFIND (see Methods). In contrast to other haplotype-based approaches<sup>3,5</sup>, SOURCEFIND uses a Bayesian model that eliminates contributions that cannot be reliably distinguished from background noise. Simulations show that SOURCEFIND has greater accuracy than other approaches used to examine sub-continental ancestry (Supplementary Note 1). For ease of visualization, we collapsed the ancestry components inferred from these 56 clusters into 35 groups, based on the genetic relatedness of the clusters (Supplementary Fig. 3).

Allele-based analyses have previously documented that broad patterns of Native American population structure are detectable in admixed Latin Americans<sup>6,7</sup>. SOURCEFIND analysis extends these results by enabling the inference of 25 Native American ancestry components across Latin America, resulting in a high-resolution picture of Native variation in the region (Figures 1B and 2A) and emphasizing the “genetic continuity” of pre-Columbian and admixed populations across the Americas. In addition, SOURCEFIND distinguishes between closely-related ancestry components from the Iberian Peninsula, as well as from the East and South Mediterranean (including individuals self-identified as Sephardic; i.e. Iberian Jews). The distribution of European ancestry in the CANDELA sample shows a sharp differentiation between Brazil and the Spanish American countries (Fig. 1C). In Brazil the predominant European sub-component matches mostly the Portugal/West-Spain reference group while in Mexico, Colombia, Peru and Chile mostly Central/South-Spanish ancestry is inferred (Figures 1C and 2B). This differentiation matches the colonial history, Portuguese migration having concentrated in Eastern South America while the Spanish settled mainly in Central America and Western South America<sup>1</sup>. The relatively small contribution inferred for the Basque and Catalan agrees with historical information documenting that Spanish migrants to America originated mainly in Southern and Central Spain<sup>8</sup>. In addition, the Brazilian sample shows substantial Italian and German ancestry, and these components concentrate in the South of the country. This pattern is consistent with the documented migration to Southern Brazil of large numbers of Germans and Italians in the late 19th century<sup>9</sup>.

To assess the time-frame of admixture between the ancestry components described above we used the program GLOBETROTTER<sup>5</sup>. Since admixture proportions in Latin Americans vary greatly, we analyzed each individual separately; simulations confirmed the accuracy of GLOBETROTTER in this setting (Supplementary Note 1). Inferred dates for events involving Iberian components had a median of 10 generations (IQR=7-13), consistent with other estimates for admixture in Latin America<sup>6,10,11</sup>. Noticeably, individuals with more recent inferred dates of admixture have greater Native ancestry (Fig. 3A, Supplementary Table 4), consistent with continuing admixture between admixed Latin Americans and unadmixed Natives, possibly as a result of the decline in Iberian immigration after the mid-17th century, concomitant with the demographic recovery of neighboring Native American populations<sup>12,13</sup>. Admixture involving the German or Italian components have a significant skew towards more recent dates than admixture involving Iberians (Fig. 3B; Wilcoxon rank-sum test one-sided p-value= $3 \times 10^{-8}$ )<sup>9</sup>, consistent with the relatively recent arrival of Germans and Italians.

SOURCEFIND finds that Sephardic/East/South Mediterranean ancestry is detectable in all the countries sampled: Brazil (1%), Chile (4%), Colombia (3%), Mexico (3%) and Peru (2%). Altogether, ~23% of the CANDELA individuals show >5% of such ancestry (Fig. 1D) and in these individuals SOURCEFIND infers this ancestry to be mostly Sephardic (7.3%), with smaller non-Sephardic East Mediterranean (3.9%) and non-Sephardic South Mediterranean (1%) contributions. Individuals with Sephardic/East/South Mediterranean ancestry were detected across Latin America (Fig. 2C). GLOBETROTTER estimates for the time since Sephardic/East/South Mediterranean admixture were not significantly different from those involving Iberian sources (Fig. 3C; Wilcoxon rank-sum test one-sided p-value>0.1). It is possible that outliers with particularly high values of Sephardic/East/South Mediterranean ancestry are descendants from recent non-European immigrants. For 19 of 42 individuals with >25% Sephardic/East/South Mediterranean ancestry genealogical information (up to grandparents) identified recent ancestry in the Eastern Mediterranean. However, no recent immigration was documented for Colombians with >5% Sephardic ancestry, despite these individuals showing the highest estimated Sephardic ancestry across

countries (10% on average, Fig. 1D). Jewish communities existed in Iberia (*Sepharad*) since roman times and much of the peninsula was ruled by Arabs and Berbers for most of the Middle Ages, by the end of which large Sephardic communities had developed<sup>14</sup>. Genetic studies have detected North and East Mediterranean ancestry in the current Spanish population, as well European admixture in the Sephardim<sup>15-17</sup>. The estimates of North and East Mediterranean (including Sephardic) ancestry in Latin Americans obtained here represent values over and above those present in our sampled present-day Spanish individuals, suggesting migration of individuals with higher levels of such ancestry to Latin America. Columbus' arrival to the New World in the late 15<sup>th</sup> century coincided with the expulsion of Jews from Iberia, with the non-Christians remaining being forced to convert to Christianity. Although these *Conversos* were forbidden from migrating to the colonies, historical records document that some individuals made the journey, in an attempt to avoid persecution<sup>14</sup>. Since this was a clandestine process, the extent of *Converso* migration to Latin America is poorly documented. Genetic studies have provided suggestive evidence that certain Latin American populations, arguably with a peculiar history, could have substantial *Converso* ancestry<sup>1,18</sup>. Our findings indicate that the genetic signature of *Converso* migration to Latin America is substantially more prevalent than suggested by these special cases, or by historical records.

The average Sub-Saharan ancestry estimated in the full CANDELA sample is ~4%, reflecting the fact that regions which historically received large numbers of African slaves are under-represented<sup>4</sup>. SOURCEFIND infers a marked predominance of the West African sub-component, particularly in the Spanish American countries (Supplementary Figures 4 and 5), consistent with previous genetic analyses, and with historical information<sup>13,19</sup>. The distribution of dates involving Sub-Saharan African admixture mostly overlaps with that for Iberian admixture, although a substantial proportion of recent dates were also inferred (Fig. 3D), possibly reflecting continuing admixture in the regions sampled. Historical information indicates some East Asian migration to Latin America, from the 19<sup>th</sup> century onwards<sup>9</sup>. SOURCEFIND estimates East Asian ancestry in the CANDELA sample to be, on average, very low (<1%) in Brazil, Chile, Colombia, Mexico, and slightly higher in Peru (1.4%). In individuals with >5% East Asian ancestry, this component is inferred to be most closely related to the Chinese and to a lesser extent the Japanese, except in Brazil where the opposite is found (Supplementary Fig. 6). GLOBETROTTER estimated dates for admixture involving an East Asian source were significantly more recent than those involving Iberian sources (median = 3, IQR 2-5 generations ago, Wilcoxon rank-sum test one-sided p-value < 10<sup>-15</sup>; Fig. 3E).

Individuals in the CANDELA sample have been characterized for a range of physical appearance features, including aspects of anthropometry, face and ear morphology, facial and scalp hair, and pigmentation (of hair, skin and eyes) (Supplementary Note 2). We evaluated the impact of sub-continental genetic ancestry on these features using linear regression. To maximize power and reduce collinearity, we focused on contrasts involving the most frequent and differentiated sub-continental ancestry components (see Methods, Fig. 1). SOURCEFIND results allowed the analysis of two contrasts. The first involved North-West Europe versus Portugal/West-Spain ancestry in the Brazilian sample. We observed a highly significant effect of this contrast on pigmentation traits (Fig. 4A-C). This observation validates our approach, as it is consistent with the latitudinal gradient in pigmentation observed within Europe, and the corresponding differentiation in allele frequencies at pigmentation genes between Northern and Southern Europeans<sup>20</sup>. The second contrast examined involved a "Central Andean" component (obtained by merging the closely related Quechua1, Quechua2, Colla and Aymara components) versus the relatively differentiated Mapuche component (Fig.1). This contrast is significantly associated in the CANDELA sample, with variation in facial features, particularly nose shape (Fig. 4A-B), lower nose

protrusion being associated with higher Mapuche ancestry (Fig. 4D). Validation analyses limited to Peru and Chile or only to Chile, using the ancestry components inferred by SOURCEFIND as well as related components obtained with ADMIXTURE or PCA (Supplementary Figures 7 and 8, Supplementary Note 3), produced similar results (Fig. 4E, Supplementary Note 4). It is noticeable that regional Native American ancestry impacts on nose shape. The Mapuche component is strongly associated with a less protruded nose (P-value  $<2 \times 10^{-5}$ ) and broader nose tip angle (P-value  $<10^{-7}$ ). This is consistent with physical anthropology analyses indicating that the Mapuche have a flatter, wider nose than Central Andean populations<sup>21</sup>. In a recent genome-wide association scan for facial features in the CANDELA sample most loci identified impacted on nose shape<sup>22</sup> and index SNPs at those loci show significantly differentiated allele frequencies between Central Andeans and the Mapuche, consistent with the phenotypic effects of the regional ancestry analyses (Supplementary Table 5). The nasal cavity is an important regulator of inhaled air temperature and humidity, and evolutionary studies suggest that nose shape has been influenced by adaptation to cold/dry versus hot/humid environments<sup>23</sup>. Since variation in altitude correlates with air temperature and humidity, it will be interesting to explore further whether the association of Central Andean ancestry with nose shape relates to altitude adaptation during Native American evolution.

The genetic signature of a wide-spread migration of *Conversos* to Latin America provides a striking example of how analyses of regional population structure can uncover poorly documented demographic history events. Furthermore, demonstrating an effect of regional Native ancestry on facial features illustrates the power of such analyses for establishing the genetic basis of geographic variation in human phenotypes, possibly in relation to local evolutionary adaptation. The ability to extract such fine-grained patterns of sub-continental genetic structure in individuals with recent ancestry from multiple sources promises a broad range of applications, particularly considering the ubiquity of recent admixture in human populations<sup>5</sup>.

## Methods:

### Genotype datasets

The CANDELA dataset (<http://www.ucl.ac.uk/candela>) consists of genotypes from 6,852 individuals ascertained in five Latin American countries (Brazil N=676, Chile N=1,891, Colombia N=1,713, Mexico N=1,288 and Peru N=1,284) (Supplementary Fig. 1). This study sample and ethical approval has been described in detail in Ruiz-Linares *et al.* 2014<sup>4</sup>. Briefly, adult individuals of both sexes were ascertained at one main recruitment site per country (Porto Alegre in Brazil, Arica in Chile, Medellín in Colombia, Mexico City in Mexico and Lima in Peru). A structured interview recorded the birthplace of volunteers and their ancestors (up to grandparents), as well as information on the language(s) spoken by them. We have previously reported genome-wide association studies based on Illumina OmniExpress chip data obtained in these individuals<sup>22,24,25</sup>.

To perform ancestry analyses in the CANDELA individuals we collated a reference population dataset from regions having potentially contributed to admixture in Latin America. We combined publicly available data with data from newly genotyped samples obtained here (Fig. 1, Supplementary Table 1, Supplementary Fig. 2). Altogether we collated data for 2,359 individuals from 117 reference populations (38 Native American, 42 European, 15 East/South Mediterranean, 15 Sub-Saharan African and 7 East Asian). Of these,

42 were newly genotyped population samples (comprising 27 Native American, 7 European and 8 East/South Mediterranean), including a total of 430 individuals. These individuals were genotyped on the Illumina HumanOmniExpress chip which includes 730,525 SNPs. PLINK v1.9<sup>26,27</sup> was used to exclude SNPs and individuals with more than 5% missing data, markers with minor allele frequency <1%, related individuals, and those who failed the X-chromosome sex concordance check. The same QC filters had been applied to the CANDELA dataset<sup>22,24,25</sup>. Individuals born outside the country were relocated when coming from one of the five countries included in this study or otherwise removed. Similar quality controls were applied to the public reference population datasets. In addition, unsupervised ADMIXTURE<sup>28</sup> analyses of reference population samples were used to identify and exclude Sub-Saharan Africans, East Asians and Europeans with less than 95% of their own continental ancestry. In the case of Native Americans, all individuals were initially retained (regardless of admixture levels), but reference individuals with less than 95% Native American ancestry were only used for haplotype phase inference. In the case of East/South Mediterranean individuals, ADMIXTURE consistently inferred Sub-Saharan African ancestry. The estimated Sub-Saharan African ancestry proportions were found to be quite homogeneous across individuals, possibly indicating relatively old shared ancestry. Based on this assumption, we excluded 4 individuals with admixture proportions deviating markedly from those observed in the population sample, suggestive of recent admixture (three Moroccans with Sub-Saharan African ancestry >40% and one Libyan with Sub-Saharan African ancestry of 79%; both of these populations have an estimated average Sub-Saharan African ancestry of ~20% +/- 3%).

After QC, the merged CANDELA + reference population dataset comprised genotypes for 546,780 autosomal SNPs in 8,647 individuals (including 6,589 Latin Americans and 2,058 individuals from the reference population samples).

### Phasing of genotype data

Phasing of the merged dataset was performed with SHAPEIT2<sup>29</sup> using default parameters. Genetic distances used were obtained from the HapMap Phase II genetic map build GRCh37<sup>30</sup>. Missing genotypes for any SNP (less than 5% after the QC) were imputed during the phasing process.

### Inference of haplotype similarity patterns

CHROMOPAINTER<sup>2</sup> was used to infer haplotype similarity (informally, “chromosome painting”) across individuals. We set-up the software to provide estimates of the proportion of DNA in every CANDELA and reference population individual (denoted recipients) that is most closely related to each reference population individual (denoted donors), allowing us to reconstruct haplotype similarity profiles for all individuals in terms of the reference samples. The recombination scaling constant  $N_e$  and the mutation parameter  $\theta$  used by CHROMOPAINTER were jointly estimated for every individual in a subset of chromosomes (1, 6, 13 and 22) with 10 Expectation-Maximization steps, starting from default values defined by the software. The average  $N_e$  and  $\theta$  values across chromosomes (weighted by chromosome size) were then used for subsequent CHROMOPAINTER runs on all autosomes ( $N_e = 290.83$  and  $\theta = 0.00038$ ). Genetic distances from the HapMap Phase II genetic map build GRCh37 were used in the CHROMOPAINTER runs. CANDELA individuals with >99% European ancestry (52 Brazilians, of which 37 reported German and 15 Italian

ancestors) or with >95% Native American ancestry (1 Colombian, 22 Mexicans, 65 Chileans and 17 Peruvians) were included amongst the donors as they may harbour ancestry components not present in our reference dataset. In Supplementary Note 5 we show how that our conclusions about ancestry are similar if these individuals are excluded from the reference dataset. In total, 157 CANDELA individuals and 1,942 reference individuals were added to the panel of donors, for a total of 2,099 samples. The remaining 116 individuals from the initial reference dataset were excluded. Of these 80 were Native Americans with less than 95% Native ancestry, and 36 were Native Americans excluded after the haplotype-based clustering analyses performed to select the reference panel for the ancestry inference, as explained in the next section.

### **Definition of homogeneous clusters of reference population individuals**

To evaluate genetic structure in the reference data, independent of population sample labels, we used fineSTRUCTURE<sup>2</sup>, a program that defines homogeneous clusters of individuals based on the similarity of the haplotype copying profiles obtained by CHROMOPAINTER. To run fineSTRUCTURE, a likelihood adjustment factor ( $c$ ) is initially calculated in order to account for the inaccurate assumption that the amount of DNA matching among individuals is independent. Using default CHROMOPAINTER settings to infer the adjustment factor, this was estimated as  $c=0.236$ . Two MCMC runs were performed using 2,000,000 iterations (sampling every 10,000). Following Leslie *et al.* 2015<sup>3</sup>, for each run the sample with maximum posterior probability was selected and an additional 100,000 hill-climbing moves were then performed to search for merges or splits that further improve the overall model likelihood<sup>2</sup>. After this procedure, fineSTRUCTURE classified individuals into 129 clusters. In order to reduce the number of clusters potentially representing sources of ancestry in Latin America, to avoid problems related to collinearity between different surrogate sources when estimating ancestry, and to facilitate interpretation of the results, we carried out the refinements described below, leading to the re-assignment of individuals from these 129 clusters into 117 “donor clusters”. Of these, 56 were considered “surrogate clusters” for inferring sub-continental ancestry in the CANDELA individuals (as described in the section “A new haplotype-based estimation of ancestry” below). The refinements were as follows:

First, we checked the consistency of the assignments of every individual into a given cluster. We excluded all individuals that were assigned to a different cluster more than 10% of the time across samples in the last 1,000,000 iterations of the two fineSTRUCTURE runs, and 5 clusters where all individuals were inconsistent across these samples. We also excluded 12 individuals assigned to their own unique clusters, and 10 small clusters made of either a small number of individuals from distant populations or from populations present in other clusters with greater numbers.

Next, we used the remaining clusters (i.e. those not set aside above) to perform an initial estimation of sub-continental ancestry in the CANDELA samples using a modification of the Non-Negative Least Squares (NNLS) regression approach<sup>3,5</sup>. We excluded individuals from 17 clusters that based on this analysis did not contribute to the CANDELA samples. Furthermore, based on the tree inferred by fineSTRUCTURE and on Total Variation Distance (TVD) (e.g. as used in Leslie *et al.* 2015<sup>3</sup>), we merged 29 remaining clusters that were difficult to distinguish from one another into 13 groups. After these steps, there were 69 clusters remaining intact from the original 129 (a subset of which became the final 56 “surrogate clusters” as described in the next paragraph).



We next took all individuals that had been excluded as described above and reclassified them into 48 clusters based on population label information. This resulted in 117 “donor clusters” that we use throughout. Supplementary Table 2 lists how individuals from the initial 129 fineSTRUCTURE clusters were classified into the 117 donor clusters. We then performed a few additional steps to define the final 56 “surrogate clusters”, starting from 69 “intact” clusters described above, using the modified NNLS regression approach<sup>3,5</sup>. In particular, we checked if closely related clusters could potentially contribute to collinearity issues in subsequent analyses or if they had complex ancestry profiles that could eventually complicate the interpretation of the results. To perform the regression analysis, the proportions of DNA that each individual from the 69 clusters matches to each donor as estimated by CHROMOPAINTER were summed across donors within each of the 117 donor groups defined above. For each individual from the 69 clusters, this produces a vector of 117 variables that we call a “copying vector”, with each variable the proportion of DNA that this individual copies from (i.e. matches to) all individuals contained in that donor group. For each of the 69 clusters, we averaged these copying vectors across all individuals assigned to that cluster, creating a unique copying vector for each of the 69 clusters. Then, for each of these 69 clusters, we performed a NNLS regression with the copying vector of that cluster as the response and the copying vectors for all 68 other clusters as predictors. From these analysis, 7 clusters (whose individuals belong to the Native American populations Uros, Kogi, Karitiana, Surui, Ticuna and Mixe (Supplementary Table 2)) with considerable levels of genetic drift (as evidenced by the amount of haplotype similarity within their own cluster and the fact that their painting profile, as interpreted by NNLS, cannot be explained as mixtures of other populations) and no contributions to the CANDELA samples were excluded; these clusters were also removed from the donors for subsequent analyses given their high amounts of genetic drift. An additional 6 clusters showing complex signals in NNLS analyses were also excluded based on the following criteria: (i) the cluster contributed to the ancestry profiles of several surrogate groups of interest and (ii) the cluster showed ancestry from more than two continental groups. For instance, in the case of (i) we excluded *Sardinia* as it was contributing high amounts (~15%) to the ancestry of *Portugal/WestSpain*, *Catalonia* and *Italy*. The best example for (ii) is *Turkey*, which was inferred to have >5% ancestry from an East Asian source and 5% from a European one. These analyses resulted in the 69 “intact” clusters being reduced to 56 “surrogate clusters” that are made of 1,444 individuals from the reference panel. Supplementary Table 3 details the individual makeup of these 56 clusters, in terms of the population sample labels. Supplementary Figure 3 shows a phylogenetic tree relating these clusters and allowing the definition of 35 “surrogate groups” based on their genetic similarity.

### **SOURCEFIND: A new haplotype-based estimation of ancestry**

The 56 surrogate clusters defined above were used for inferring the ancestral population contributions to admixture in Latin America. We generated copying vectors for each CANDELA individual and for each individual included in the 56 surrogate clusters by summing the proportion of DNA that every individual matched to individuals from the 117 donor clusters defined in the previous section. To cope with differences in surrogate cluster size and improve resolution, we modelled the copying vector of each CANDELA individual as a weighted mixture of the copying vectors from the surrogates<sup>3,5</sup>. To do so, we introduce a model-based approach we term SOURCEFIND, which outperforms the NNLS approach taken in Leslie *et al.* 2015<sup>3</sup>. Below we describe the SOURCEFIND algorithm.

Let  $l^r \equiv \{l_1^r, \dots, l_D^r\}$  be the copying vector describing the total genome length (in cM) that a recipient individual (or group)  $r$  copies from each of the  $d \in [1, \dots, D] = 117$  donor clusters as inferred by CHROMOPAINTER (Note that copying vectors can also be averaged across recipients to perform the analysis in groups). Here for any  $r$ ,  $\sum_{d=1}^D l_d^r = C$ , where  $C$  is equal to the total genome length of DNA (in cM), and we further define  $f_d^r \equiv \frac{l_d^r}{C}$ . Henceforth we let  $r$  denote a CANDELA individual, and  $s$  denote a surrogate cluster. In the latter case,  $l_d^s$  represents an average across all individuals from that surrogate cluster.

We assume that:

$$Pr(l^r | l^1, \dots, l^S, C, \beta^r) = \text{Multinomial} \left( C; \sum_{s=1}^S [\beta_s^r f_1^s], \dots, \sum_{s=1}^S [\beta_s^r f_D^s] \right)$$

Where  $\beta^r \equiv \{\beta_1^r, \dots, \beta_S^r\}$  are the mixture coefficients we aim to infer and every  $s \in [1, \dots, S] = 56$  represents a surrogate cluster used to describe the ancestry of group  $r$ . In practice, often all the donor clusters are used as surrogates, so that  $S = D$ . However, in our case the surrogates are a subset of the donors so that  $S < D$ .

We take a Bayesian approach to inferring  $\beta^r$ , further assuming the following:

$$\begin{aligned} Pr(\beta^r | \lambda) &= \text{Dirichlet}(\lambda_1, \dots, \lambda_S), \\ Pr(\lambda) &= \text{Uniform}(0,10). \end{aligned}$$

For each recipient  $r$ , we wish to sample the mixing coefficients  $\{\beta_1^r, \dots, \beta_S^r\}$  based on their posterior probabilities conditional on  $l \equiv \{l^r, l^1, \dots, l^S\}$ . We do so using the following Markov Chain Monte Carlo (MCMC) technique. We start with an initial value of  $\lambda(0) = 0.5$  and sample our initial values of  $\beta^r(0) \equiv \{\beta_1^r(0), \dots, \beta_S^r(0)\}$  from the prior distribution Dirichlet  $(\lambda(0), \dots, \lambda(0))$ . Then for  $m \in [1, \dots, M]$ :

Update  $\beta^r(m) \equiv \{\beta_1^r(m), \dots, \beta_S^r(m)\}$  using a Metropolis-Hastings (M-H) step:

- i. Randomly sample  $Y \sim \text{Unif}(0,0.1)$ .
- ii. Randomly sample a surrogate  $s_x$  and set  $\beta_{s_x}^r(m) = \beta_{s_x}^r(m-1) + Y/5$ . For numerical stability, if  $\beta_{s_x}^r(m) > 1 - 1e^{-7}$ , set  $\beta_{s_x}^r(m) = 1 - 1e^{-7}$ . Repeat this for 4 additional randomly sampled (with replacement) surrogates  $s_x$ .
- iii. Randomly sample a surrogate  $s_x$  and set  $\beta_{s_x}^r(m) = \beta_{s_x}^r(m-1) - Y/5$ . For numerical stability, if  $\beta_{s_x}^r(m) < 1 - 1e^{-7}$ , set  $\beta_{s_x}^r(m) = 1e^{-7}$ . Repeat this for 4 additional randomly sampled (with replacement) surrogates  $s_x$ .
- iv. For all other surrogates  $s \in [1, \dots, S]$ , excluding the randomly sampled set above, set  $\beta_s^r(m) = \beta_s^r(m-1)$ .
- v. Re-scale  $\sum_{s=1}^S \beta_s^r(m) = 1.0$ .
- vi. Accept  $\beta^r(m)$  with probability  $\min(\alpha, 1.0)$ , where:

$$\alpha = \frac{Pr(l^r | l^1, \dots, l^S, C, \beta^r(m)) Pr(\beta^r(m) | \lambda(m-1))}{Pr(l^r | l^1, \dots, l^S, C, \beta^r(m-1)) Pr(\beta^r(m-1) | \lambda(m-1))}$$

Update each  $\lambda_s(m)$  for  $s = 1, \dots, S$  using a M-H step:

- i. Propose a new  $\lambda_s(m)$  from a Normal ( $\lambda_s(m - 1), sd = 0.2$ ).
- ii. Automatically reject if  $\lambda_s(m) \notin [0,10]$ .
- iii. Otherwise accept  $\lambda_s(m)$  with probability  $\min(\alpha, 1.0)$ , where:

$$\alpha = \frac{Pr(\beta^r(m)|\lambda(m))}{Pr(\beta^r(m)|\lambda(m-1))}$$

For large  $M$ , this algorithm is guaranteed to converge to the true posterior distribution of the  $\beta^r$ 's (e.g. Gamerman 1997<sup>31</sup>). In practice, we used  $M=200,000$ , sampling every 1,000 iterations. Also, for each recipient individual  $r$ , we combined results across 50 independent runs of the above procedure, extracting the estimates with the highest posterior probability in each run and then taking a weighted (by posterior probability) average of these 50 estimates. We refer to the final estimates of  $\{\beta_1^r, \dots, \beta_S^r\}$ , weighted by posterior values, as our inferred proportions of ancestry for individual  $r$  conditional on this set of  $S$  surrogates. This approach differs from the mixture model procedure described in<sup>3,5,32-34</sup> in that it assumes that  $l^r$  is multinomial distributed and solves for  $\beta^r$  using a Bayesian approach rather than a non-negative least squares optimization. The model is similar to the one described in<sup>35</sup>, but introduces new improvements in the way that  $\lambda$  is estimated and in the MCMC proposal procedure.

The accuracy and robustness of the ancestry estimations obtained by SOURCEFIND and NNLS were evaluated using simulations mimicking Latin American admixture (Supplementary Note 1).

SOURCEFIND is available upon request from [g.hellenthal@ucl.ac.uk](mailto:g.hellenthal@ucl.ac.uk)

### Estimation of the number of generations since admixture

The times and sources of major admixture events were inferred using the program GLOBETROTTER<sup>5</sup>. GLOBETROTTER tests for evidence of one or more pulses of admixture between two or more ancestral groups, and dates these admixture events and infers the genetic make-up of the admixing groups involved. Due to the recent nature of intermixing in the Americas, admixture times and proportions may vary substantially across CANDELA individuals. Therefore we tested each individual separately, restricting this analysis to the 6,352 individuals inferred by SOURCEFIND to have ancestry from more than one surrogate cluster.

For each haploid genome of each individual, we used 10 random samples of genome-wide local matching to donor clusters per haplotype as provided by the CHROMOPAINTER analysis described above. For each CANDELA individual, we ran GLOBETROTTER including as surrogates only the subset of  $\leq 56$  clusters that contributed  $>1\%$  to that individual, as inferred by SOURCEFIND. For each CANDELA individual, GLOBETROTTER categorized admixture inference into one of three types: (i) one date of admixture involving two sources, (ii) one date of involving more than two sources (suggestive of a admixture among multiple genetically different groups within a short time span), and (iii) multiple dates of admixture between two or more sources (not necessarily the same two), suggesting a more complicated history but which GLOBETROTTER attempts to describe as two major pulses of admixture.

Altogether, for 55.4% of the CANDELA individuals (3519/6352) GLOBETROTTER inferred a single admixture event between two source groups, while in 44.6% of the CANDELA individuals (2833/2378) a more complex admixture was inferred. This could

consist of more than two groups admixing (Supplementary Fig. 9) and/or multiple dates of admixture (Fig. 3B, Supplementary Table 6). For simplicity, the inferred admixture history of these latter individuals was described as two distinct events, with each event characterised as having two admixing groups and a single date of admixture. In total GLOBETROTTER inferred 9,185 such admixture events (Supplementary Table 6). For simplicity, we represent the two admixing sources using GLOBETROTTER's "best-guess" results, which describes each admixing source by the single (included) surrogate group out of 56 that is inferred to be most genetically similar to that (unknown) admixing source group.

To convert the time estimates obtained by GLOBETROTTER (in generations) into years, we used the formula  $y=1990-28*(g+1)$ , where  $y$  is the year of admixture, 1990 is the mean birth year in CANDELA individuals,  $g$  the estimated admixture time (in generations), and taking 28 years as the generation time.

### **Testing for differences in the distributions of inferred admixture dates for different source groups**

In Figure 3, we plot histograms of inferred dates for each of the major geographic labels "Iberia", "NorthWestEurope & Italy", "East Mediterranean & Sephardic", "Sub-Saharan African (SSA)" and "East Asia". These plots contain the inferred dates for all admixture events (out of 9,185) that involved a inferred source group categorized under that major geographic label, with:

"Iberia": CanaryIslands, Portugal/WestSpain, CentralSouthSpain, CentralNorthSpain, Basque and Catalonia.

"NorthWestEurope & Italy": Italy1 and NorthWestEurope1.

"East Mediterranean & Sephardic": Sephardic1, EastMediterranean1 and EastMediterranean2.

"Sub Saharan Africa": WestAfrica1, WestAfrica2, WestAfrica3, EastAfrica1, EastAfrica2, Namibia and SouthAfrica.

"East Asia": Japan, ChinaHan, China/Vietnam1 and China/Vietnam2.

We used "wilcox.test" in R<sup>36</sup> to perform a one-sided Wilcoxon rank-sum test (also known as a Mann-Whitney U test) to test the alternative hypothesis that the distribution of admixture dates for each geographic label  $X = \{ \text{"East Asia"}, \text{"NorthWestEurope \& Italy"}, \text{"East Mediterranean \& Sephardic"}, \text{"SSA"} \}$  is skewed towards more recent dates relative to the "Iberia" geographic label, versus the null hypothesis that distributions are the same. Though they may represent genuine admixture events, for these tests and the histograms of Figure 3 we removed events with an inferred date of 1. This was done both to avoid such dates dominating inference due to their high frequency (8% of all events in Iberia have inferred dates of 1, with East Asia = 21%, NorthWestEurope & Italy = 6%, East Mediterranean & Sephardic = 10%, SSA = 13%) and because such events have been interpreted as evidence of "no admixture" in past applications of GLOBETROTTER (e.g. <sup>5</sup>). For the Wilcoxon rank-sum test, we further excluded individuals with  $\leq 5\%$  ancestry from  $X$  and individuals with dates  $\geq 30$  generations to avoid admixture events that occurred prior to colonial-era migrations. In addition, this analysis assumes each inferred event is an independent observation, even though some individuals have two inferred events. However, we note that conclusions and trends do not change if we restrict to one inferred event per individual (results omitted), e.g. by excluding individuals who infer multiple dates of admixture (i.e. case (iii) described in "Estimation of number of generations since admixture"

above) and only including the more strongly signaled event in individuals who infer more than two sources of admixture at the same time (i.e. case (ii) described in “Estimation of number of generations since admixture” above).

### **Association of sub-continental ancestry with physical features**

We recorded 28 physical appearance traits, by physical examination of the volunteers and/or by examining facial photographs. These traits have been described in detail previously<sup>4,22,24,25</sup> and brief definitions are provided in Supplementary text 5.

To evaluate the phenotypic effect of sub-continental ancestry components defined by SOURCEFIND we used linear regression. Since these components are (negatively) correlated with other major continental ancestries, using them directly would cause confounding in the linear model. We therefore performed linear regression analysis including a contrast between subcontinental ancestry components. To maximize power, we defined three criteria for making these contrasts: (i) each component tested should have at least 10% frequency in a country (ii) the two sub-continental ancestry components contrasted should add up to at least half of the total continental ancestry in a country and (iii) the components contrasted should show a relatively high genetic differentiation.

These criteria only allowed one contrast to be made based on the European components (Fig. 1): that between North-West Europe and Portugal/West-Spain in Brazil. In addition, merging the closely related Quechua1, Quechua2, Colla and Aymara into a “Central Andean” component, enabled a Native American contrast based on the SOURCEFIND analysis. Similar components were defined by Principal Component (PC) 7 (Supplementary Fig. 8) and by ADMIXTURE at K=7 (Supplementary Fig. 7), which we tested for consistency.

The basic regression model tested was:

Phenotype ~ Age + Sex + Socioeconomic status + Total Sub Saharan African ancestry + Total European ancestry + Native component contrast,  
or,

Phenotype ~ Age + Sex + Socioeconomic status + Total Sub Saharan African ancestry + Total Native American ancestry + European component contrast.

For facial traits, BMI was included as a covariate. When doing a multi-country analysis we also used country as dummy variable. To reduce variability from other continental ancestries, we excluded individuals with high Sub Saharan African or East/South Mediterranean ancestry and individuals with >1% East Asian ancestry.

### **Differences in allele frequencies of GWAS hits in Mapuche and Central Andean populations**

To test whether allele frequencies differed between individuals with Mapuche versus Central Andean ancestry at loci previously identified as being associated with facial features<sup>22</sup>, we first inferred the allele frequencies at these loci in each of the Mapuche and Central Andean populations. As we have relatively few reference individuals with Mapuche and Central Andean ancestry, we inferred allele frequencies by combining these reference samples with admixed Candela individuals that were inferred to carry the appropriate Native ancestry at these loci.

To do so, we used the software RFMix<sup>37</sup> to infer local continental ancestry in the subset of phased Candela individuals described earlier. Three continental reference panels

(consisting of phased haplotypes for 107 IBS, 101 YRI and 125 Native American samples) were used for this purpose. RFMix assigns local continental ancestry to each allele of each Candela haplotype, allowing for errors in genotyping, slight admixture in the reference samples, etc. Thus for each allele of each haplotype, it produces two files of relevance – the local ancestry at that site, and the ‘putative’ allele at that site (after ‘fixing’ any such errors).

Using SOURCEFIND sub-continental ancestry proportions, two different sets of Candela individuals were selected to obtain allele frequencies for Central Andes and Mapuche groups. For each set, all individuals had >10% inferred ancestry from that Native group, with <1% combined inferred ancestry from all other Native groups and <1% inferred East Asian ancestry. For all individuals in a group, for each locus, all alleles that had local Native ancestry (as inferred by RFMix) were aggregated to estimate the allele frequency for that group. Allele frequencies thus obtained for Central Andes were very similar to the allele frequencies obtained from 49 surrogate individuals of the Central Andes group who were inferred to have >99% Native ancestry ( $r^2 > 0.99$ ) (the number of surrogate individuals with >99% Native ancestry for the Mapuche group wasn’t large enough for such a comparison).

Allele frequencies were thus obtained for the index SNPs (among the chip data) of all the six genomic regions identified in Adhikari *et al.* 2016<sup>22</sup>. A t-test was used to assess whether the allele frequencies were significantly different in Central Andes vs. Mapuche individuals. The FDR (false discovery rate) procedure was used to control the Type-I error rate at 0.05 level. After the FDR procedure, all SNPs showed a significant difference in allele frequency between Central Andes & Mapuche. Furthermore, for each SNP, the allele with a higher frequency in Central Andes compared to Mapuche had the same direction of effect (same signs of regression coefficient beta) for that allele in the GWAS as compared to the regression coefficient (beta, Fig. 4B) between the CentralAndes-Mapuche contrast and the trait, for all traits that are associated at a genome-wide significant or suggestive significant level with the SNP.

**Acknowledgments:** We are very grateful to the volunteers for their enthusiastic support for this research. We thank Alvaro Alvarado, William Arias, Mónica Ballesteros Romero, Ricardo Cebrecos, Miguel Ángel Contreras Sieck, Francisco de Ávila Becerril, Joyce De la Piedra, María Teresa Del Solar, Gastón Macín, William Flores, Martha Granados Riveros, Rosilene Paim, Ricardo Gunski, Sergeant João Felisberto Menezes Cavalheiro, Major Eugênio Correa de Souza Junior, Wendy Hart, Ilich Jafet Moreno, Claudia Jaramillo, Paola León-Mimila, Francisco Quispealaya, Diana Rogel Diaz, Ruth Rojas and Vanessa Sarabia, for assistance with volunteer recruitment, sample processing and data entry. We acknowledge the institutions that kindly provided facilities for the assessment of volunteers: Escuela Nacional de Antropología e Historia and Universidad Nacional Autónoma de México (México); Universidade Federal do Rio Grande do Sul (Brazil); 13° Companhia de Comunicações Mecanizada do Exército Brasileiro (Brazil); Pontificia Universidad Católica del Perú, Universidad de Lima and Universidad Nacional Mayor de San Marcos (Perú). Ethics approval was obtained from Universidad Nacional Autónoma de México (México), Universidad de Antioquia (Colombia), Universidad Peruana Cayetano Heredia (Perú), Universidad de Tarapacá (Chile), Universidade Federal do Rio Grande do Sul (Brazil) and University College London (UK). We also thank the National Laboratory for the Genetics of Israeli Populations (<http://yoran.tau.ac.il/nlgip/>) and Dr. David Gurwitz for making

available DNA samples. We thank Chris Tyler-Smith and Caroline Costedoat for comments on the manuscript. This work was funded by grants from the Leverhulme Trust (F/07 134/DF to A.R.-L.), BBSRC (BB/I021213/1 to A.R.-L.), Wellcome Trust/Royal Society (098386/Z/12/Z to G.H.), Universidad de Antioquia (CODI sostenibilidad de grupos 2013- 2014 and MASO 2013-2014), Conselho Nacional de Desenvolvimento Científico e Tecnológico, Fundação de Amparo à Pesquisa do Estado do Rio Grande do Sul (Apoio a Núcleos de Excelência Program) and Fundação de Aperfeiçoamento de Pessoal de Nível Superior. V.G. is supported by Fundação para a Ciência e Tecnologia (FCT) and Programa Operacional Potencial Humano (POCH), through the grant SFRH/BPD/76207/2011. IPATIMUP integrates the i3S Research Unit, which is partially supported by FCT. Y.X. was supported by The Wellcome Trust (098051). J.C.C.-D. was supported by a doctoral scholarship from COLCIENCIAS-Colombia.

**Author contributions:** J.C.C.-D., K.A., J.M.-R., M.F.-G., G.H. and A.R.-L. performed the analyses. G.H. developed SOURCEFIND. J.C.C.-D., K.A., G.H. and A.R.-L. wrote the paper with input from co-authors. All other authors contributed to volunteer recruitment or collection of data. A.R.-L. coordinated the study.

**Competing financial interests:** The authors declare no competing financial interests.

**Data availability:** Raw genotype or phenotype data are not publicly sharable due to ethics restrictions. GWAS summary statistics from the CANDELA consortium have been deposited at GWAS central.

**Software availability:** SOURCEFIND is available upon request from [g.hellenthal@ucl.ac.uk](mailto:g.hellenthal@ucl.ac.uk).

**Corresponding authors:** [andresruiz@fudan.edu.cn](mailto:andresruiz@fudan.edu.cn) (A.R.-L.); [g.hellenthal@ucl.ac.uk](mailto:g.hellenthal@ucl.ac.uk) (G.H.)

## FIGURES

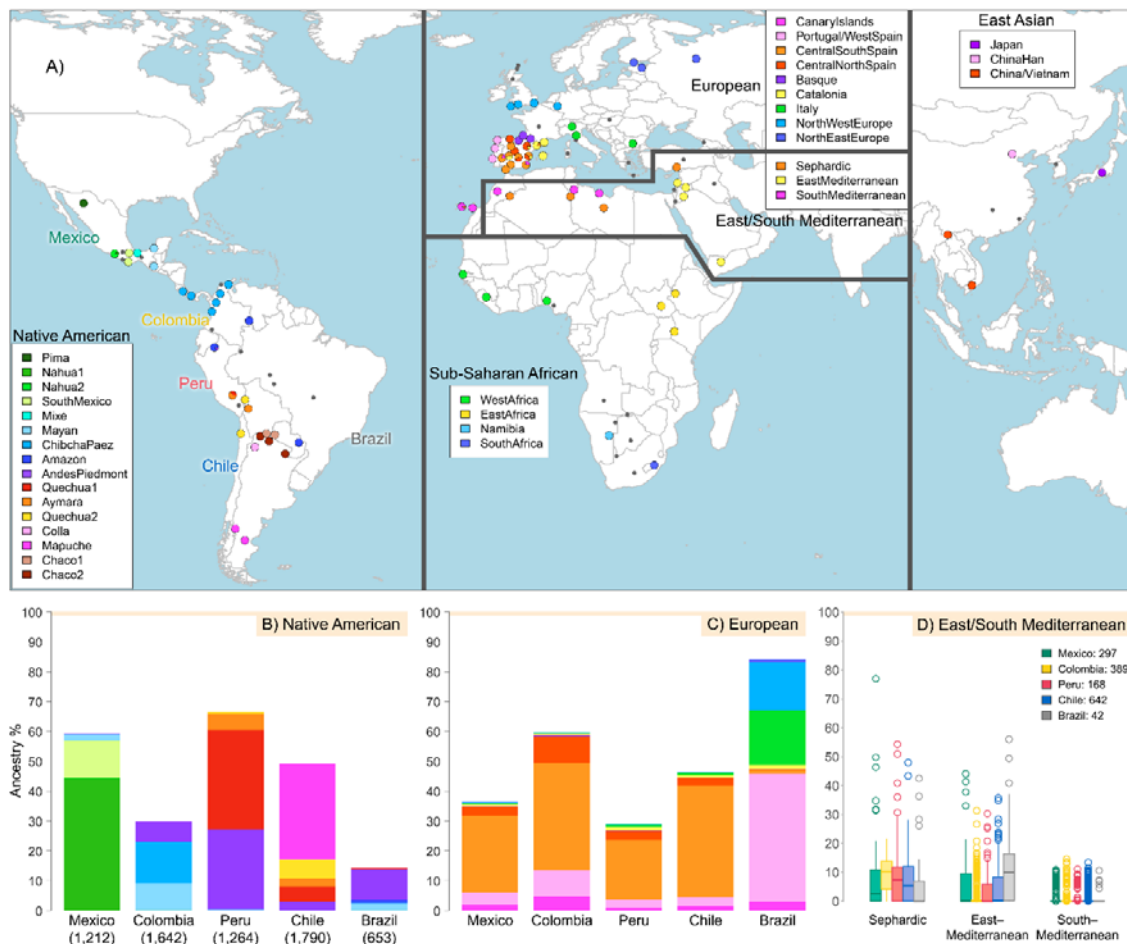


**Fig. 1.** Reference population samples, fineSTRUCTURE groups and SOURCEFIND ancestry estimates for the five Latin American countries examined. (A) Colored pies and grey dots indicate the approximate geographic location of the 117 reference population samples studied. These samples have been subdivided on the world map into five major biogeographic regions: Native Americans (38 populations), Europeans (42 populations), East/South Mediterraneans (15 populations), Sub-Saharan Africans (15 populations) and East Asians (7 populations). The coloring of pies represents the proportion of individuals from that sample included in one of the 35 reference groups defined using fineSTRUCTURE (these groups are listed in the color-coded insets for each region; Supplementary Fig. 2). The grey dots indicate reference populations not inferred to contribute ancestry to the CANDELA sample. Panels (B) and (C) show, respectively, the estimated proportion of sub-continental Native American and European ancestry components in individuals with >5% total Native American or European ancestry in each country sampled (the stacked bars are color-coded as for the reference population groups shown in the insets of panel (A)). Panel (D) shows boxplots of the estimated sub-continental ancestry components for individuals with >5% total Sephardic/East/South Mediterranean ancestry. In this panel colors refer to countries as for the colored country labels shown in (A).



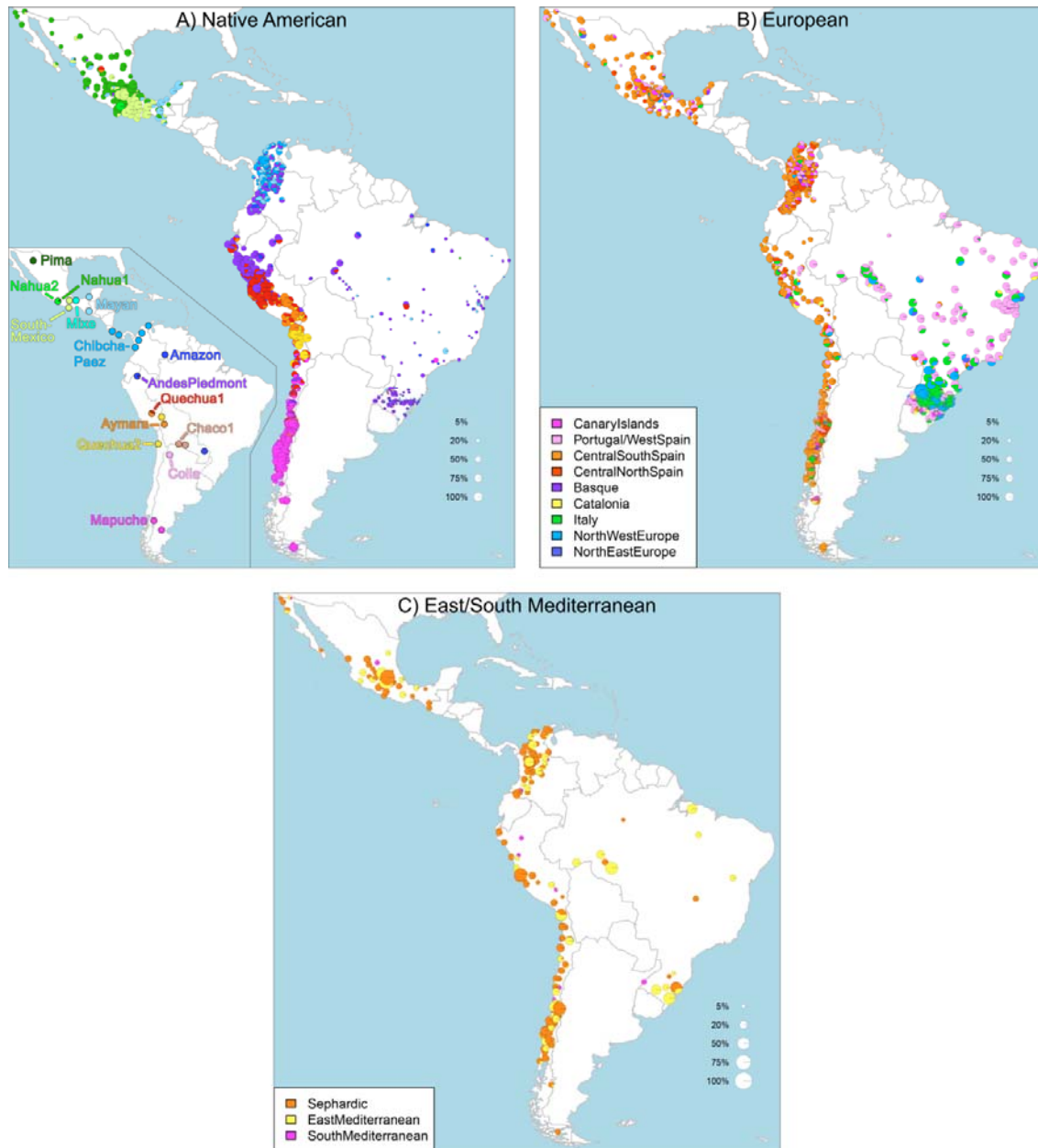


**Fig. 2.** Geographic variation of Native American (**A**), European (**B**), and East/South Mediterranean (**C**) ancestry sub-components in Latin American individuals. Each pie represents an individual with pie location corresponding to birthplace. Since many individuals share birthplace, jittering has been performed based on pie size and how crowded an area is. Pie size is proportional to total continental ancestry and only individuals with >5% of each continental ancestry are shown. Coloring of pies represents the proportion of each sub-continental component estimated for each individual (color-coded as in Fig. 1; *Chaco2* does not contribute >5% to any individual and was excluded). Pies in panel (C) have been enlarged to facilitate visualization.

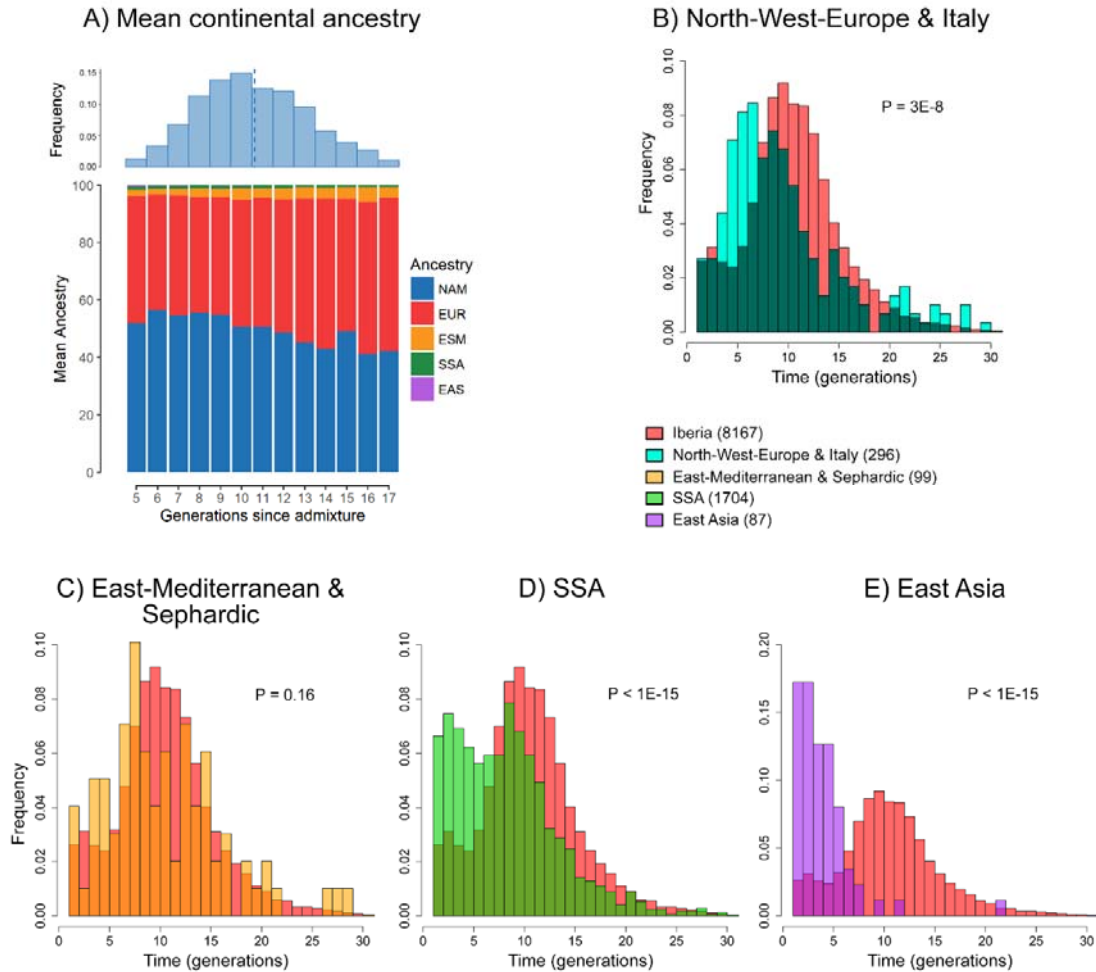


**Fig. 3.** Times since admixture estimated using GLOBETROTTER. Panel (A) Top: frequency distribution of admixture times for individuals in which a single admixture event between Native and European sources was inferred (dashed line indicates the mean). Bottom: mean continental ancestry (%) as a function of time since admixture among these individuals. Only time bins including  $>20$  individuals are shown. (NAM= Native American, EUR = European, ESM = East/South Mediterranean, SSA= Sub-Saharan African, EAS = East Asian). Panels (B-E) show contrasts of the distribution of admixture times involving Iberian or other sources: (B) North-West European/Italian (C) East Mediterranean/Sephardic (D) Sub-Saharan African and (E) East Asian.  $P$ -values for the contrasts of the distributions are from a one-sided Mann-Whitney U test.

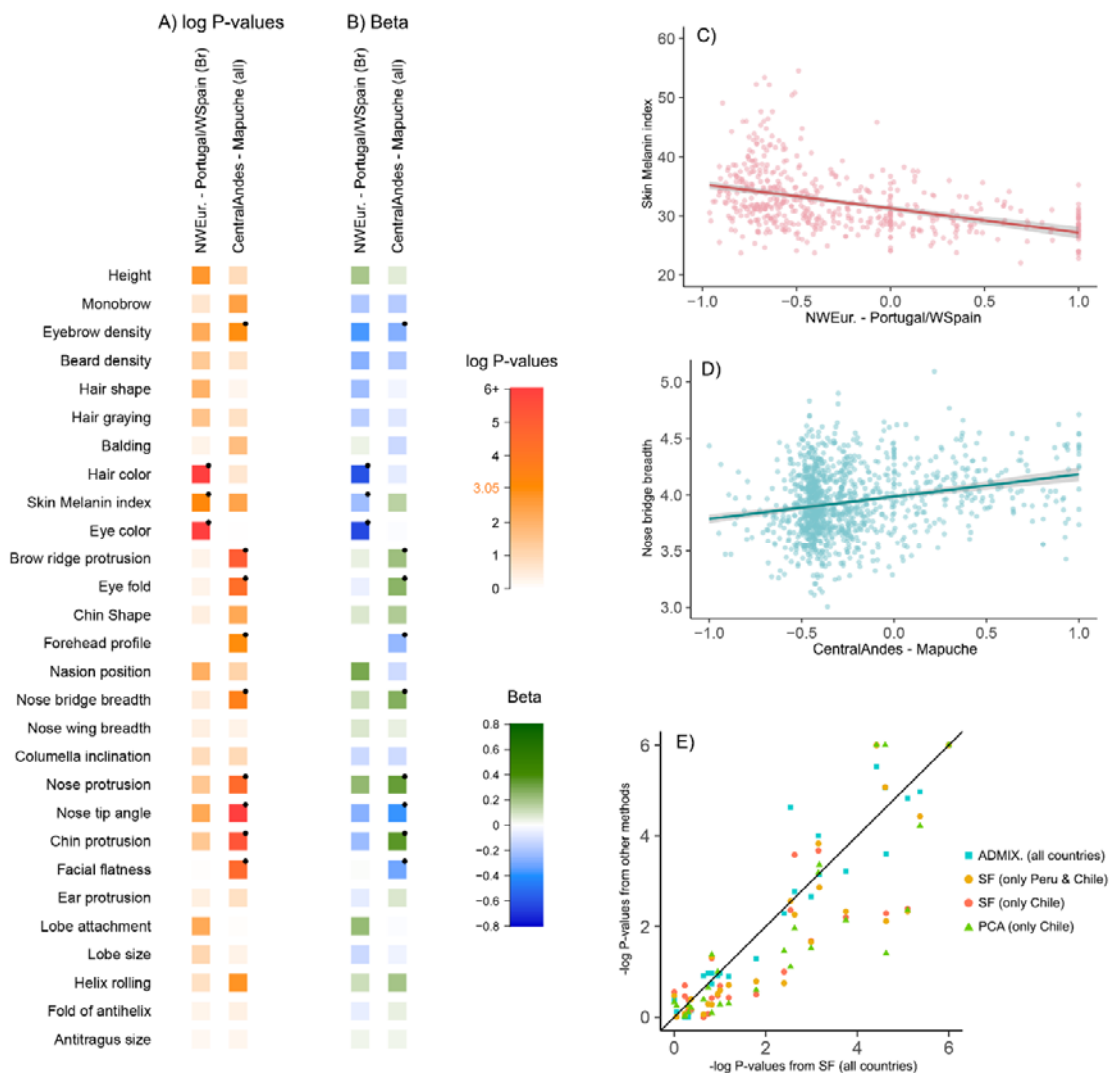


**Fig. 4.** Effect of sub-continental genetic ancestry on physical appearance. **(A)** Regression  $-\log$  P-values for 28 traits (Supplementary Material) against the contrast between two sub-continental ancestry components estimated by SOURCEFIND. The left column shows results for the Portugal/West-Spain versus North-West Europe contrast in the Brazilian sample (Br). The two right columns present the contrast between Central Andes versus Mapuche ancestry in the full CANDELA sample. **(B)** Regression coefficients (Betas) in units of SD for the contrasts in **(A)**. In panels **(A)** and **(B)** color intensity reflects variation in  $-\log$ -P values or beta coefficients, as indicated on the scale. Bonferroni-corrected significant values are highlighted with a dot ( $-\log$  P-value threshold of 3.05 for  $\alpha=0.05$ ). Panels **(C)** and **(D)** display scatterplots and regression lines (with 95% confidence intervals) for two traits showing significant association with variation in sub-continental ancestry: skin melanin index in Brazilians **(C)** and nose bridge breadth in Chileans and Peruvians **(D)**; Y-axis is in Procrustes units). **(E)** Scatterplot of  $-\log$  P-values from follow-up analyses of the regression of physical traits on the Central Andes versus Mapuche ancestry contrast. The X-axis refers to  $-\log$  P-values from the primary analyses (using SOURCEFIND (SF) estimates and data for all individuals, as shown in the second column of **(A)**). The Y-axis refers to  $-\log$ -P values from four other regression analyses: using SOURCEFIND (SF) estimates restricted to Peruvian and Chilean individuals, or only to Chileans; using related ancestry components defined by: ADMIXTURE (ADMIX., at  $K=7$ ) in all the CANDELA data, or by PCA (PC 7),

in an analysis limited to Chileans (Supplementary Note 4, Supplementary Fig. 7-8). Sample sizes: all data  $N = 5,794$ , Peruvians and Chileans  $N = 2,594$ , Chileans  $N = 1,542$ .

## REFERENCES

- 1 Adhikari, K., Chacon-Duque, J. C., Mendoza-Revilla, J., Fuentes-Guajardo, M. & Ruiz-Linares, A. The Genetic Diversity of the Americas. *Annual Review of Genomics & Human Genetics* **18** (2017).
- 2 Lawson, D. J., Hellenthal, G., Myers, S. & Falush, D. Inference of population structure using dense haplotype data. *PLoS genetics* **8**, e1002453, doi:10.1371/journal.pgen.1002453 (2012).
- 3 Leslie, S. *et al.* The fine-scale genetic structure of the British population. *Nature* **519**, 309-314, doi:10.1038/nature14230 (2015).
- 4 Ruiz-Linares, A. *et al.* Admixture in Latin America: geographic structure, phenotypic diversity and self-perception of ancestry based on 7,342 individuals. *PLoS genetics* **10**, e1004572, doi:10.1371/journal.pgen.1004572 (2014).
- 5 Hellenthal, G. *et al.* A genetic atlas of human admixture history. *Science* **343**, 747-751, doi:10.1126/science.1243518 (2014).
- 6 Wang, S. *et al.* Geographic patterns of genome admixture in Latin American Mestizos. *PLoS genetics* **4**, e1000037 (2008).
- 7 Moreno-Estrada, A. *et al.* The genetics of Mexico recapitulates Native American substructure and affects biomedical traits. *Science* **344**, 1280-1285 (2014).
- 8 Boyd-Bowman, P. Patterns of Spanish Emigration to the Indies until 1600. *Hispanic American Historical Review* **66**, 580-604 (1976).
- 9 Kent, R. B. *Latin America : regions and people (second edition)*. (Guilford Press, 2016).
- 10 Moreno-Estrada, A. *et al.* Reconstructing the population genetic history of the Caribbean. *PLoS genetics* **9**, e1003925, doi:10.1371/journal.pgen.1003925 (2013).
- 11 Homburger, J. R. *et al.* Genomic Insights into the Ancestry and Demographic History of South America. *PLoS genetics* **11**, e1005602, doi:10.1371/journal.pgen.1005602 (2015).
- 12 Burkholder, M. A. & Johnson, L. L. *Colonial Latin America*. (Oxford University Press, 2003).
- 13 Salzano, F. M. & Bortolini, M. C. *The Evolution and Genetics of Latin American Populations*. (Cambridge University Press, 2001).
- 14 Sachar, H. M. *Farewell España : the world of the Sephardim remembered*. (Knopf, 1994).
- 15 Adams, S. M. *et al.* The genetic legacy of religious diversity and intolerance: paternal lineages of Christians, Jews, and Muslims in the Iberian Peninsula. *American journal of human genetics* **83**, 725-736, doi:10.1016/j.ajhg.2008.11.007 (2008).
- 16 Botigue, L. R. *et al.* Gene flow from North Africa contributes to differential human genetic diversity in southern Europe. *Proceedings of the National Academy of Sciences of the United States of America* **110**, 11791-11796, doi:10.1073/pnas.1306223110 (2013).
- 17 Crawford, M. H. & Campbell, B. C. *Causes and Consequences of Human Migration: An Evolutionary Perspective*. (Cambridge University Press, 2012).
- 18 Velez, C. *et al.* The impact of Converso Jews on the genomes of modern Latin Americans. *Human genetics* **131**, 251-263, doi:10.1007/s00439-011-1072-z (2012).
- 19 Kehdy, F. S. *et al.* Origin and dynamics of admixture in Brazilians and its effect on the pattern of deleterious mutations. *Proceedings of the National Academy of Sciences of the United States of America* **112**, 8696-8701, doi:10.1073/pnas.1504447112 (2015).

- 20 Frost, P. The Puzzle of European Hair, Eye, and Skin Color. *Advances in Anthropology* **4**, 78-88 (2014).
- 21 Comas, J. *Antropologia de los pueblos iberoamericanos*. (Biblioteca Universitaria Labor, 1974).
- 22 Adhikari, K. *et al.* A genome-wide association scan implicates DCHS2, RUNX2, GLI3, PAX1 and EDAR in human facial variation. *Nature communications* (2016).
- 23 Zaidi, A. A. *et al.* Investigating the case of human nose shape and climate adaptation. *PLoS genetics* **13**, e1006616, doi:10.1371/journal.pgen.1006616 (2017).
- 24 Adhikari, K. *et al.* A genome-wide association scan in admixed Latin Americans identifies loci influencing facial and scalp hair features. *Nature communications* **7**, 10815, doi:10.1038/ncomms10815 (2016).
- 25 Adhikari, K. *et al.* A genome-wide association study identifies multiple loci for variation in human ear morphology. *Nature communications* **6**, 7500, doi:10.1038/ncomms8500 (2015).
- 26 Chang, C. C. *et al.* Second-generation PLINK: rising to the challenge of larger and richer datasets. *GigaScience* **4**, 7, doi:10.1186/s13742-015-0047-8 (2015).
- 27 Purcell, S. *et al.* PLINK: a tool set for whole-genome association and population-based linkage analyses. *American journal of human genetics* **81**, 559-575, doi:10.1086/519795 (2007).
- 28 Alexander, D. H., Novembre, J. & Lange, K. Fast model-based estimation of ancestry in unrelated individuals. *Genome research* **19**, 1655-1664, doi:10.1101/gr.094052.109 (2009).
- 29 Delaneau, O., Zagury, J. F. & Marchini, J. Improved whole-chromosome phasing for disease and population genetic studies. *Nature methods* **10**, 5-6, doi:10.1038/nmeth.2307 (2013).
- 30 International HapMap, C. *et al.* A second generation human haplotype map of over 3.1 million SNPs. *Nature* **449**, 851-861, doi:10.1038/nature06258 (2007).
- 31 Gamerman, D. *Markov chain Monte Carlo : stochastic simulation for Bayesian inference*. (Chapman & Hall, 1997).
- 32 Hofmanova, Z. *et al.* Early farmers from across Europe directly descended from Neolithic Aegeans. *Proceedings of the National Academy of Sciences of the United States of America* **113**, 6886-6891, doi:10.1073/pnas.1523951113 (2016).
- 33 Montinaro, F. *et al.* Unravelling the hidden ancestry of American admixed populations. *Nature communications* **6**, 6596, doi:10.1038/ncomms7596 (2015).
- 34 van Dorp, L. *et al.* Evidence for a Common Origin of Blacksmiths and Cultivators in the Ethiopian Ari within the Last 4500 Years: Lessons for Clustering-Based Inference. *PLoS genetics* **11**, e1005397, doi:10.1371/journal.pgen.1005397 (2015).
- 35 Broushaki, F. *et al.* Early Neolithic genomes from the eastern Fertile Crescent. *Science*, doi:10.1126/science.aaf7943 (2016).
- 36 Team, R. C. R: A language and environment for statistical computing. (2013).
- 37 Maples, B. K., Gravel, S., Kenny, E. E. & Bustamante, C. D. RFMix: a discriminative modeling approach for rapid and robust local-ancestry inference. *American journal of human genetics* **93**, 278-288, doi:10.1016/j.ajhg.2013.06.020 (2013).